Turkish Journal of Electrical Engineering & Computer Sciences

http://journals.tubitak.gov.tr/elektrik/

Research Article

Turk J Elec Eng & Comp Sci
(2018) 26: 393 – 406

doi:10.3906/elk-1703-224

Model-free approach based on intelligent PD controller for vertical motion reduction in fast ferries

Mounia TICHERFATINE*, Zhu QIDAN
College of Automation, Harbin Engineering University, Harbin, Heilongjiang, P.R. China

Received: 19.03.2017 • **Accepted/Published Online:** 14.11.2017 • **Final Version:** 26.01.2018

Abstract: A new model-free approach was investigated to control two moving flaps and a T-foil of a fast ferry traveling in the head sea. Considered as a highly perturbed system, fast ferries in sea waves suffer from the undesirable effects of pitch and heave motions causing severe vertical accelerations that lead to the discomfort of passengers who then experience seasickness. To appropriately control this multivariable system, a model-free control strategy was adopted. An augmented PD controller with compensating terms resulting from an online identification of an ultralocal model of the system was designed. Relying only on input–output data and using online numerical differentiation based on a fast estimation technique, a nonphysical model was designed and continuously updated to capture all the unknown system dynamics, uncertainties, and perturbations. The resulting controller, known as an intelligent PD (iPD) controller, has been proven to be of a reduced design complexity but able to cope with the system's changing characteristics under high perturbations. The robustness to parameter variations was analyzed and compared to a classic PD controller's performance. The results showed that good reductions in the system's vertical motions and seasickness were obtained with a low computational cost. Moreover, the iPD successfully exhibited very robust behavior based on its model-free property when changing the system parameters and the operating velocity.

Key words: Model-free control, intelligent PD, T-foil, flap, ship control

1. Introduction

Fast ferries navigating during sea wave disturbances will encounter complicated degrading motion. This can lead to the variation or the degradation of the ship's navigational speed. Meanwhile, the safety of the passengers is also affected by exposing them to seasickness. These undesirable motions are the main cause limiting the development of high-speed ferries. Large pitch and heave oscillations in the vertical plane of fast ships become more and more significant for a ship's ability to navigate and provide safety with the increasing wave frequency encountered, which may cause different dynamic instability problems [1,2]. As a solution, research studies have been carried out to alleviate these unpleasant motions by means of different devices with associated control schemes. These systems are commonly known as antipitching devices, such as T-foils and flaps [3]. Providing a lift force when changing their angle, these devices can temper the wave's effect on the ship when they are adequately moved. Some experimental studies on heave and pitch motions were carried out on a scaled-down model of a fast ferry for testing the motion reduction of active control systems [4–6]. Classical PD and PID controllers relying on a linear model of a fast ferry were used for smoothing the motion of the ship when using such antipitching devices [7,8]. However, as these controllers are tuned with a simple (linear) model, they could

*Correspondence: m.ticherfatine@gmail.com

render poor results when a process has a large operating domain. Moreover, it may affect the robustness due to poor modeling and/or disturbances. With the development of the control techniques, the classical PID control is unable to satisfy particular requests, especially in a highly perturbed system such as ships in sea waves. However, designing complex control systems to deal with the nonlinearities of the model involves complete knowledge of the system's dynamics and its perturbations, thus producing many new challenges [9]. Therefore, control schemes with low computational cost and easy-to-use and theoretically understandable controllers are needed. Those controllers need the efficiency to deal with unmodeled dynamics of complex processes and disturbances. In this paper, a possible solution to this problem is proposed based on some new results in the framework of model-free control (MFC) [7].

MFC has been proven to be a simple but very efficient nonlinear feedback technique for unknown or partially known dynamics [10,11]. This recent technique has been formalized to cope with general types of nonlinearities while maintaining the PID's reduced computational cost by employing a so-called intelligent PID (iPID). A precise relationship between the iPID and PIDs was presented in the work of d'Andréa-Novel et al., which highlighted the straightforwardness of tuning the iPID gains [12]. In this study, the MFC-based iPD was adopted to deal with fast ferry vertical motion reduction in a head sea by means of two moving flaps below the transom and a moving T-foil near the bow. The MFC is based on an ultralocal model approximation of the system dynamics. This model estimation is continuously updated based only on the knowledge of the input-output attitude. This provides a very effective tool to understand the system dynamics behavior while under perturbation. It is important to mention that the term "intelligent" already exists in the literature in the work of Aström et al., but with a different meaning [13]. Aström and coworkers gave some efficient rules for an optimal tuning of the PID's gains, which was considered as an intelligent way for the tuning. Later on, a variety of tuning methods were introduced, including artificial intelligent algorithms to get to optimal or self-tuned gains [14]. However, the intelligent PD controllers discussed in this paper depend on the local estimation of the system dynamics with uncertainties and disturbances. The added "intelligent" term to the well-known PD controller contains all the structural information of the system dynamics to be canceled. Exhibiting smarter functioning and adding more robustness to the classic PDs with reduced mathematical complexity, the MFC has been successfully applied to our system. Our study is organized as follows: the process model of a fast ferry equipped with two rotating flaps and a T-foil is proposed. The effect of the waves on the ship's vertical motions and their accelerations is introduced where motion sickness incidence (MSI) is defined as an evaluation tool of a passenger's discomfort. The MFC strategy is then proposed and the estimation of the ultralocal model of the system is established using a fast estimation technique. The iPD control law design is then explained to control the multivariable system in a random head sea. Finally, the designed controller is tested and compared to a classic PD controller to demonstrate the efficiency of this new control strategy.

2. Process model

An aluminum-made deep V hull fast ferry was studied and the principal parameters are listed in Table 1. The fast ferry's vertical dynamics are essentially pitch and heave motions causing high vertical accelerations that lead to the passengers' discomfort when suffering from seasickness. Extensive works on modeling ship dynamics have been done in the literature. A model of heaving and pitching motions of the fast ferry has been established by process identification [15,16]. For each ship's speed and sea state number the model is a set of four transfer functions relating forces and moments to pitch and heave motions. For instance, the transfer functions corresponding to a speed of 40 knots and the SSN4 predominant frequencies of encounter are given by [5]:

Table 1. Principal parameters of the fast ferry.

Parameters	Value
Draft	2.405 m
Dead weight	475 t
Length	110 m
Beam	14.69 m

$$F2H\,(s) = \frac{0.000157\left(s^2 + 0.82s + 1.74\right)}{(s^2 + 0.6495s + 1.196)(s^2 + 0.9805s + 2.767},$$

$$M2H\,(s) = \frac{0.00000166s\,(s + 0.21)}{(s^2 + 0.6495s + 1.196)\,(s^2 + 0.9805s + 2.767)},$$

$$F2P\,(s) = \frac{0.00000342\,(s + 0.22)}{(s^2 + 0.6495s + 1.196)\,(s^2 + 0.9805s + 2.767)},$$

$$M2P\,(s) = \frac{0.000000207(s2 + 0.82s + 1.91)}{(s^2 + 0.6495s + 1.196)(s^2 + 0.9805s + 2.767)}.$$

The model can be used safely in the corresponding predominant frequency encounter range where the parameter identification was performed. Experimental results of the vertical motion responses to sinusoidal waves showed that large vertical motions occur when the ratio of the wavelength λ by the ship's length L is in the interval of [1,2] [8].

The high-speed ferry is equipped with submerged antipitching devices. A T-foil is placed near the bow and two moving flaps are below the transom as shown in Figure 1. These actuators are used to reduce the motions of the ship in the vertical plane when moving them in a proper way in response to each encountered random wave. The parameters of the proposed actuators are listed in Table 2.

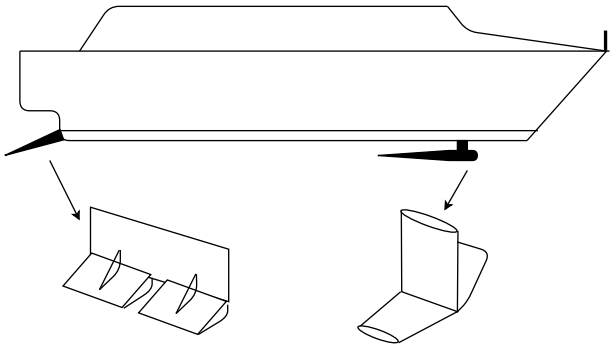

Figure 1. T-foil and flaps location on the ship.

The forces and moments generated by an actuator are a function of its angle of attack and the ship's speed, described by the following equations [3,17]:

$$F = \frac{1}{2}\rho A U^2 C_L \delta, \tag{1}$$

Table 2. Flap and T-foil characteristics.

Parameters	Flap	T-foil (one wing)
Span	4.8 m	3 m
Chord	1.1 m	2.25 m
Area	5.5 m^2	6.75 m^2
Max. angle	15°	±15°
Lift coefficient	9.19×10^{-3} KN/°/m^2/$knot^2$	6.9×10^{-3} KN/°/m^2/$knot^2$
Max. rotational speed	13.5 °/s	13.5°/s
Distance to the CG	41.6 m	58.4 m
Response time	1.2 s from 0° to 15°	2 s from –15 ° to 15°

$$M = \frac{1}{2}\rho A U^2 C_L \delta x, \tag{2}$$

where C_L, ρ, A, δ, and x are the lift coefficient, the fluid density, the area of the actuator, the effective angle of the actuator, and the distance of the actuator to the CG, respectively.

A change in the angle δ results in a change in the flow field providing a generation of the lift forces. The T-foil rotation angle is limited to [(–15°,15°)], the flap is free to move [(0° ,15°)], and their rotational speed is limited to [(–13.5°/s, 13.5°/s)] [3].

The process model of pitch and heave motions of the fast ferry equipped with the T-foil and the two flaps during wave disturbances is shown in Figure 2.

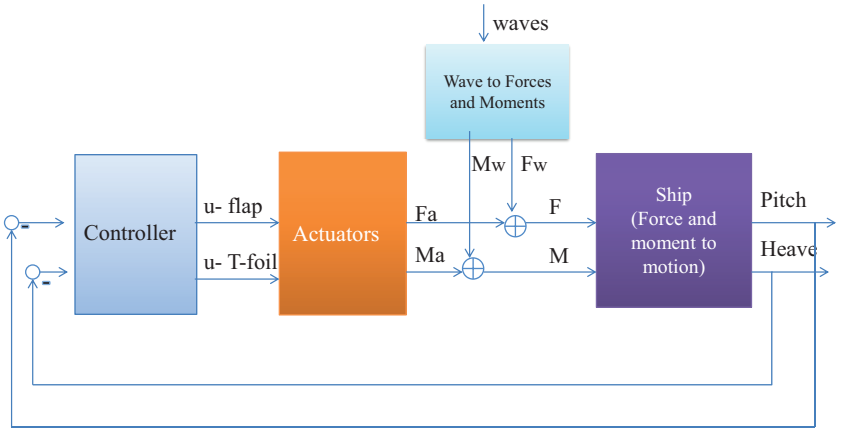

Figure 2. Process model of the ship with actuators under wave disturbances.

The effect of wave disturbances on a ship is introduced as wave-generated moments and forces, M_w and F_w, respectively. The controlled actuators provide lift moments and forces, M_a and F_a, respectively, to counteract both M_w and F_w. The resulting force and moment, F and M, respectively, will be translated by the ship into pitch and heave motions. Indeed, this is a multivariable process with two control inputs, u_{flap} and u_{T-foil}, when the waves are considered as perturbations to the system.

To simulate a wave's disturbances acting on the hull, the Pierson–Moscowitz wave spectrum was chosen and its power spectral density is defined as follows:

$$S(w) = \frac{8.11\times10^{-3}g^2}{w^5} exp\left(-\frac{3.11}{h^2_{1/3}\, w^4}\right) \tag{3}$$

where $S(w)$ is the spectrum of the wave amplitude, w is the wave frequency, and $h_{1/3}$ is the significant wave height corresponding to a specified sea state number (SSN).

The amplitude of the irregular wave can be obtained by the following equation:

$$W = \sum_{i=1}^{N} \sqrt{2S(\omega_i)\Delta\omega}\cos(\omega_i + \varepsilon_i) \tag{4}$$

where ε_i is the random phase angle of the irregular wave that varies from 0 to 2π [18].

The heaving forces and pitching moments' disturbances of the random waves with a significant height of 1.8 m acting on the hull are presented in Figure 3.

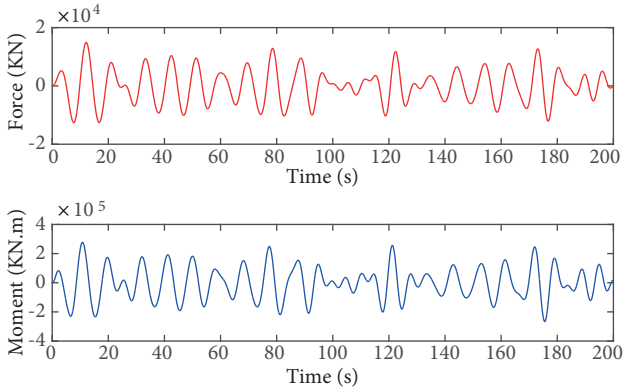

Figure 3. Wave-generated forces and moments acting on the hull at SSN4.

Here, for example, are the transfer functions used to generate forces (W2F) and moments (W2M) from the wave height at a ship speed of 40 knots:

$$W2F = \frac{698s^5 + 724.8s^4 + 15840s^3 + 5948s^2 + 59260s - 1913}{s^6 + 1.93s^5 + 9.135s^4 + 10.81s^3 + 17.02s^2 + 7.537s + 2.984} \tag{5}$$

$$W2M = \frac{327800s^4 + 628200s^3 + 193200s^2 + 4289000s - 1189000}{s^6 + 2.526s^5 + 912.92s^4 + 22.75s^3 + 38.53s^2 + 32.93s + 9.166} \tag{6}$$

3. Motion sickness and vertical acceleration

The MSI is defined as the percentage of passengers getting sick after 2 h of motions. A mathematical model of the MSI was obtained using the following expression [19]:

$$MSI = 100\left[0.5 \pm erf\left(\frac{\pm log_{10}(|a_v|/g \mp \mu_{MSI})}{0.4}\right)\right] \tag{7}$$

where erf is the error function, $|a_v|$ is the vertical acceleration at a measuring point, and μ_{MSI} is given by the following empirical expression:

$$\mu_{MSI} = -0.819 + 2.32\,(log_{10}w_e)^2 \tag{8}$$

where ω_e is the frequency of the wave encounter depending on the sea state as well as the ship's velocity, which is calculated for the head sea as:

$$w_e = w + \frac{w^2}{g}U \tag{9}$$

Since an increase in speed increases the MSI, decreasing the speed could be necessary to avoid passenger discomfort. In this case, the use of the actuators is of significant importance to minimize the MSI while sustaining the high speed of the ship. Moreover, the research of motion sickness by O'Hanlon et al. showed that motion's acceleration in the vertical plane is the main cause in a cumulative way of undesirable effects on passengers [19]. The frequencies of vertical acceleration that most easily cause motion sickness are around 1 rad/s. Additionally, the passengers sitting near the bow experience much higher vertical accelerations than those sitting near the CG of the ship. Thus, in our study, the vertical accelerations will be evaluated at the worst place where a passenger can sit. Thus, seasickness has its highest value originating from the vertical acceleration at 40 m forward from the CG, and at that point the vertical acceleration is the worst and is called the "worst vertical acceleration" (WVA). The WVA can be computed by:

$$WVA = \frac{\partial^2 h(t)}{\partial t^2} - 40\frac{\pi}{180}\frac{\partial^2 p(t)}{\partial t^2} \tag{10}$$

where $h(t)$ and $p(t)$ are the heave and pitch motions of the ferry, respectively.

4. Model-free control

Model-free control is a quite recent approach to nonlinear control that was introduced by Fliess et al. [10,20]. The input-output behavior of the system is implicitly described within its operating range by a finite-dimensional differential equation (11):

$$E\left(y,\dot{y},\ldots,y^n,u,\dot{u},\ldots,u^m\right) = 0. \tag{11}$$

Eq. (11) is replaced by an ultralocal model valid within a short time interval:

$$y^{(v)} = F + \alpha u, \tag{12}$$

where α is a nonphysical constant that is determined by the operator to ensure the desired control performances. The differentiation order v is also an operator choice, but it is generally chosen to be 1 or 2 in the model-free control literature [10–12]. F captures the unknown dynamics and perturbation in the input-output behavior and it is identified in real time from the signals u and y.

The ultralocal model can be seen as an approximated model for system dynamics valid for a short period of time that allows a real-time update. This approach attempts the simplification of the nonlinear control by discarding the need for a global and complex nonlinear model. The numerical value of F must be updated every short period T since Eq. (12) is valid for a short time window. Using the knowledge of the input u and the measurement of the output y, F can be estimated based on the online parameter identification techniques described in the following section.

4.1. Numerical estimation

Applying the Laplace transform to the ultralocal model described by Eq. (12), with the assumption that F is constant over a short period of time we get:

$$s^2Y(s) - sy(0) - \dot{y}(0) = \frac{F}{s} + \alpha U(s) \tag{13}$$

Differentiating with respect to s in order to eliminate $\dot{y}(0)$:

$$2Y(s)+s^2\frac{d}{ds}Y(s)-y(0)=-\frac{1}{s^2}F+\alpha\frac{d}{ds}U(s) \tag{14}$$

Differentiating Eq. (14) one more time in order to eliminate $y(0)$:

$$2Y(s)+4s\frac{d}{ds}Y(s)+s^2\frac{d^2}{ds^2}Y(s)=\frac{2}{s^3}F+\alpha\frac{d^2}{ds^2}U(s) \tag{15}$$

We multiply Eq. (15) by $\frac{1}{s^3}$ to eliminate any time derivatives and create low-pass filters for corrupting noises thanks to the iterated integrals:

$$2\frac{1}{s^3}Y(s)+4\frac{1}{s^2}\frac{d}{ds}Y(s)+\frac{1}{s}\frac{d^2}{ds^2}Y(s)=\frac{2F}{s^6}+\alpha\frac{1}{s^3}\frac{d^2}{ds^2}U(s) \tag{16}$$

Then, transforming back into the time domain using the inverse transformation rules:

$$\frac{a}{s^r}, r\geq 1, a\in C \longleftrightarrow a\frac{t^{r-1}}{(r-1)!}.$$

The remaining terms are transformed using the Cauchy formula for repeated integration:

$$\frac{1}{s^r}\frac{d^n}{ds^n}Y(s)\longleftrightarrow\frac{(-1)^n}{(r-1)!}\int_0^t(t-\tau)^{r-1}\tau^n y(\tau)d\tau.$$

Finally we get:

$$F=\frac{60}{t^5}\int_0^t\left(t^2 6t\tau+6\tau^2\right)y(\tau)\,d\tau\frac{30\alpha}{t^5}\int_0^t(t-\tau)^2\tau^2 u(\tau)\,d\tau \tag{17}$$

Changing the integration borders to a small fixed-length window T, we get the final expression for the algebraic estimator of the piecewise constant function F:

$$F=\frac{60}{T^5}\int_0^T\left(T^2-6T\tau+6\tau^2\right)y(t-\tau)\,d\tau\frac{30\alpha}{T^5}\int_0^T(T-\tau)^2\tau^2 u(t-\tau)\,d\tau \tag{18}$$

4.2. Controller design

Based on the numerical knowledge of F previously estimated, the control law is calculated as a cancellation of the influence of the resultant disturbance and the unknown dynamics terms $F(t)$ plus a closed-loop stabilizing term:

$$u(t)=-\frac{F(t)}{\alpha}-\frac{-y^{*(v)}(t)+\epsilon(e(t))}{\alpha} \tag{19}$$

where $e=y-y^*$ is the output error.

y^* is the reference signal of the vertical motion, which is equal to 0.

Combining Eqs. (12) and (19), we get:

$$e^{(v)}(t)+\epsilon(e(t))=0, \tag{20}$$

where $\epsilon\left(e\left(k\right)\right)$ is an appropriate function selected such that asymptotic stability is ensured:

$$e\left(t\right)=0 \tag{21}$$

To clarify Eq. (20), we choose v = 2 and $\epsilon(e)$ was chosen to be a PD control law. The iPD controller then results and the control input of the feedback is expressed as:

$$u=\frac{1}{\alpha}(-F\left(t\right)+\ddot{y}^{*}-K_{p}e-K_{d}\dot{e}). \tag{22}$$

K_p and K_d are the usual tuning proportional and derivative gains.

Eq. (21) becomes a linear differential equation of the error where the selection of Kp and Kd is direct to ensure stable closed-loop dynamics:

$$\ddot{e}+K_{d}\dot{e}+K_{p}e=0. \tag{23}$$

By choosing $K_d=2p$ and $K_p=p^2$ $;p\in R^{+}$, Eq. (23) results in a stable closed-loop dynamics with two real negative poles equal to $-p$. This is a major benefit when compared to the tuning of classic PIDs.

As summarized in Figure 4, the designed controller will be used to control the flaps and the T-foil in order to reduce the pitch and heave motions of the fast ferry. The control signals will be expressed as:

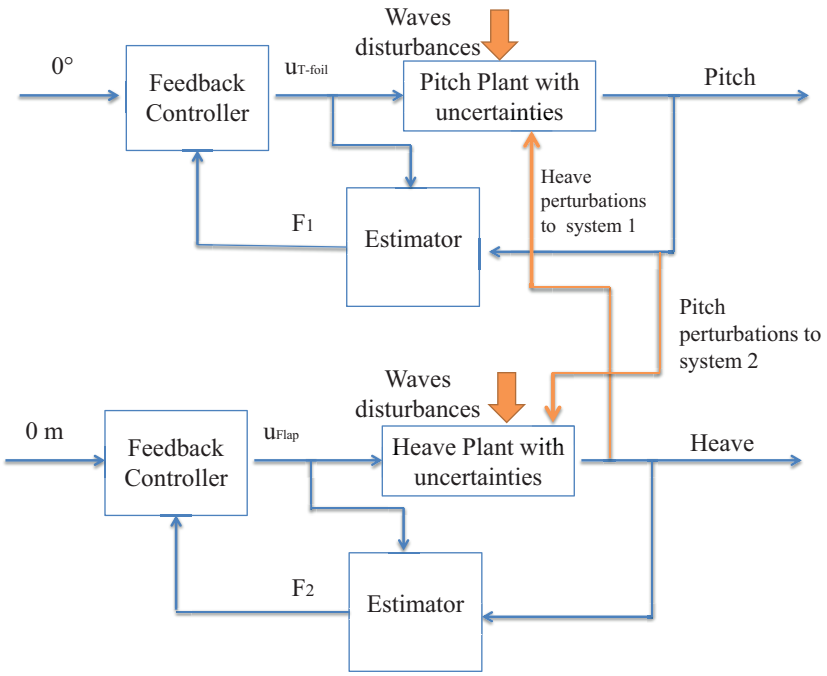

Figure 4. MFC scheme.

$$u_{Flap}=\frac{1}{\alpha_{1}}\left(-F_{1}\left(t\right)+\ddot{y}_{heave}^{*}-K_{p1}e_{heave}-K_{d1}\dot{e}_{heave}\right) \tag{24}$$

$$u_{T-foil}=\frac{1}{\alpha_{2}}\left(-F_{2}\left(t\right)+\ddot{y}_{pitch}^{*}-K_{p2}e_{pitch}-K_{d2}\dot{e}_{pitch}\right) \tag{25}$$

α_1,α_2 are the nonphysical constants determined to ensure the desired control performances of the heave and the pitch control loops, respectively.

Note here that although there is a certain degree of interaction between the pitch and heave motions, the system can be considered as two SISO systems according to [21]. The control input u_{Flap} is paired to the heave motion and u_{T-foil} is paired to the pitch motion. Also, the iPD controller can handle the interactions between pitch and heave if present by considering that the two loops are disturbances to each other. Every controller is directly designed using its proper input-output data where the system contains all the information concerning the actual dynamics.

5. Results and discussion of the numerical experiments

Numerical experiments of the fast ferry equipped with two manipulated devices were implemented, and the command signals for the flaps and the T-foil are u_{Flap} and u_{T-foil} as in Eqs. (24) and (25), respectively. Random sea waves are a perturbation to the system. White Gaussian noise was added to the output as sensor noise to obtain a complete model of the controlled system in its operational environment. To highlight the superiority of our controller, a classic PD controller has also been applied to our system. The parameters of the classic PD controller, K_p and K_d, were tuned to obtain an optimal desired performance and are listed in Table 3. The estimation of the ultralocal model in the algebraic identification of Eq. (18) was performed through a time window of T = 0.4 s. The decision for the sample time T was a result of a trade-off: the smaller T is, the more precise is the estimation and the larger is the effect of noise. The gains of the iPD are directly selected according to Eq. (23) and listed in Table 3. The constants α_1 and α_2 are obtained by trial and error until a good closed-loop performance is achieved.

Table 3. Controller parameters.

Gains	Kp_1	Kd_1	Kp_2	Kd_2	α_1	α_2
PD	160	53	90	34	-	-
iPD	40^2	80	20^2	40	10^5	10^7

The results at a speed of 40 knots in head sea and the predominant frequency of SSN4 are presented in Figures 5–10. Figures 5 and 6 present the pitch and heave motions of the ferry without control and once with the PD controller and then with the iPD. It is clear that the reduction in motion with the iPD is higher than that obtained with the classic PD. Figure 5 shows the effect of noise on the pitch motion response. Noises are viewed

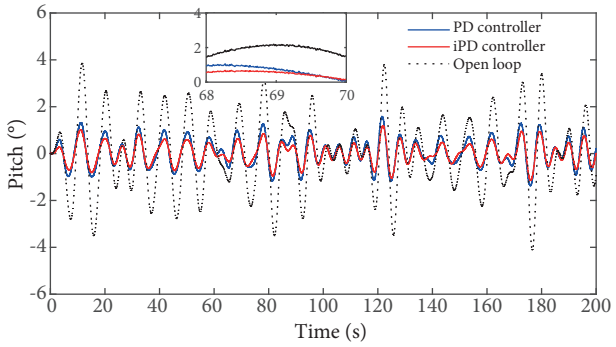

Figure 5. Pitch response at 40 knots and SSN4.

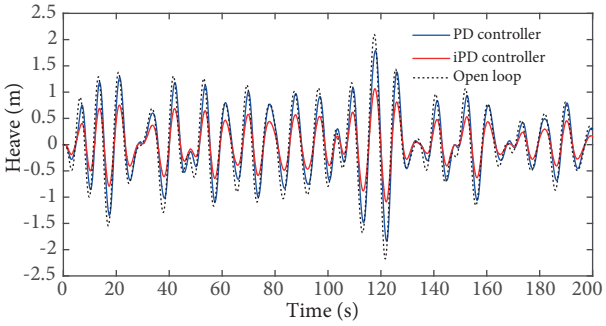

Figure 6. Heave response at 40 knots and SSN4.

as quick fluctuations and they are therefore attenuated by the low-pass filters thanks to the iterated integrals. As we can see, the iPD controller is able to achieve the desired performances in the presence of measurement noises and it is therefore effective and robust to the noises. Figure 7 represents the different forces and moments

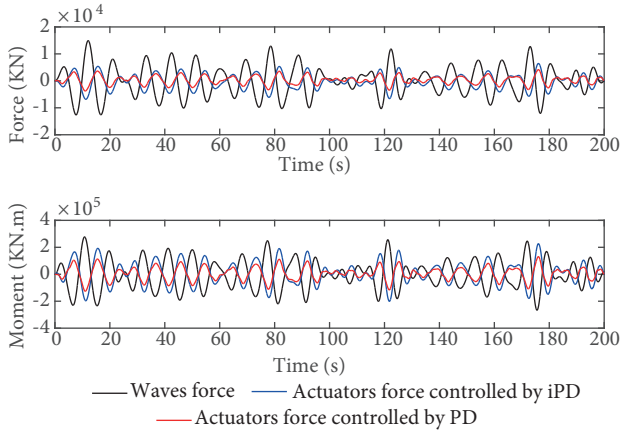

Figure 7. The different forces and moments acting on the hull.

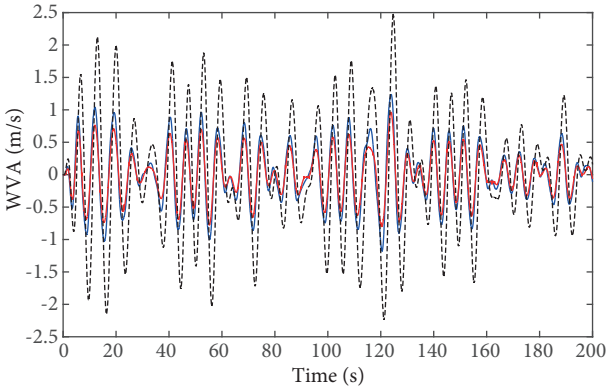

Figure 8. WVA response at 40knots and SSN4.

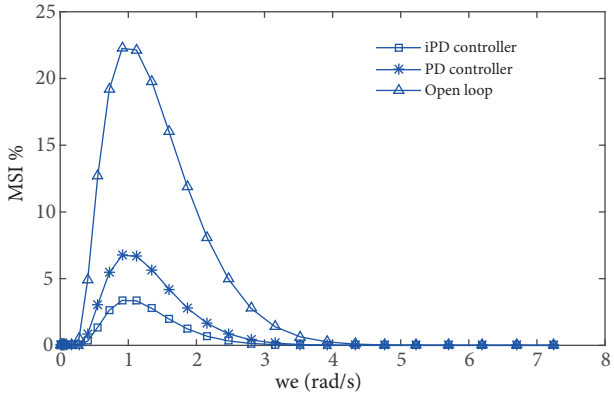

Figure 9. MSI percentages at 40 knots and SSN4.

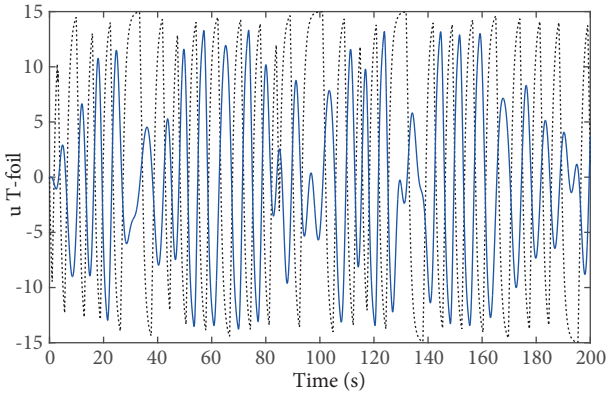

Figure 10. T-foils opening angle of PD controller (dashed line) and iPD (solid line).

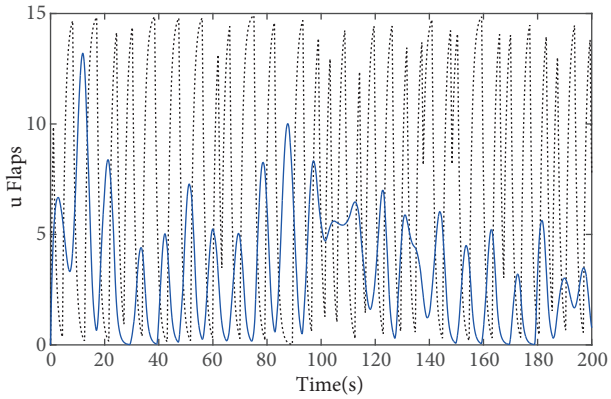

Figure 11. Flaps opening angle of PD controller (dashed line) and iPD (solid line).

acting on the hull. The actuators when controlled by the iPD provide the necessary forces and moments in a more effective way to contract the effect of wave's forces and moments. Moreover, the WVA signals, presented in Figure 8, show a significant attenuation when using the PD with a mean value of 0.41 m/s^2. However, the iPD controller performs better than the classic PD with a mean vertical acceleration of 0.30 m/s^2. Hence, as shown in Figure 9, a better MSI value was recorded using the iPD from 25.8% without control to only 4.2% compared to 8.31% of MSI using the PD controller. This is highly positive for a passenger's comfort and permits increasing the operational capabilities of the ship. It is also interesting to compare the performances of the designed controller with results in the literature, such as the report of Diaz et al. when designing a controller based on quantitative feedback theory [5]. The results showed, after a long and complicated process for designing the controller (based on linear model of the process), that the achieved reduction in MSI is slightly improved by 6% better than the PD performances. On the other hand, the iPD controller achieved a performance improvement of 20% better than the PD controller. The added intelligent term $-\frac{F(t)}{\alpha}$ to the well-known PD structure compensated the effect of the random height of the wave's disturbances. In other words, in the MFC, the local model is reidentified at each sample time T, where the influence of the updated resultant disturbance and the unknown dynamics terms can be canceled with the use of the added term $-\frac{F(t)}{\alpha}$, leading to a better performance, enhanced dynamic behavior, and attenuated perturbations. Thus, the iPD has greater robustness against disturbances through random wave perturbations. Besides, as shown in Figures 10 and 11, the actuators follow the control law without saturation and can handle the control effort limits very well.

5.1. Robustness to changing parameters

As is known, ship parameters in sea wave disturbances are highly dependent on the motion's amplitude and frequency. Thus, an MFC approach that does not rely on any parametric model is a solution. In order to show the robustness throughout the model uncertainties and changes in the ship model parameters, a modification in a range up to 30% in the system parameters was performed without any new calibration of the PD or iPD gains. The obtained results are presented in Figures 12 and 13.

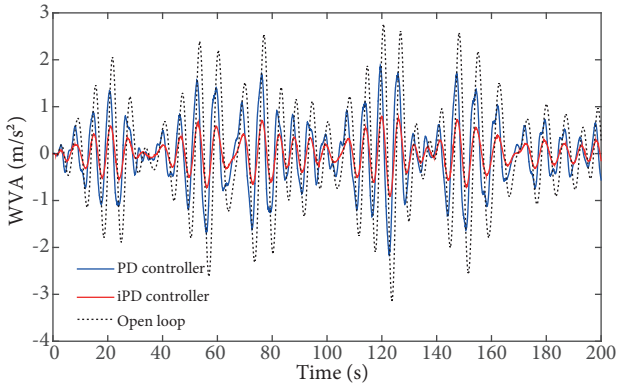

Figure 12. WVA responses with changing model parameters.

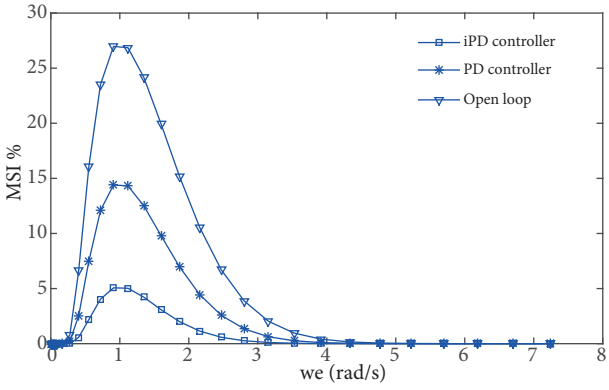

Figure 13. MSI percentages with changing model parameters.

Clearly, Figures 12 and 13 show a deterioration of the performance of the classic PD with a mean WVA of 0.56 m/s^2 and 14% of MSI, whereas the performances of the iPD remained good with a mean WVA of 0.33 m/s^2 and 4.8% of MSI. We also noted that the PD controller does not adapt to the change in the plant while

the iPD is showing sufficient control capability even if the given system coefficients have changed. This is a very important result relying on a very simple nonphysical model that can improve the control performance in a larger operating domain. We have confirmed the superiority of the iPD over the PD in the sense that there is no need to adjust the control gains when the system parameters change. Thus, the intelligent controller is more reliable against parameter variations and disturbances and has a model-free property.

5.2. Robustness to change in velocity

Table 4 lists the reduction in the MSI for both controllers at three different working speeds (20, 30, and 40 knots). This time the PD was tested twice: first without retuning the PD parameters and secondly with a gain scheduling scheme of the appropriate nominal plant related to each speed while the iPD controller's gains were maintained fixed. According to Table 4, the reductions in the MSI achieved with the retuned PD are higher than those obtained with the nonretuned PD, which is the expected result. The gain scheduling scheme is optimally tuned for the corresponding operating points. However, even by retuning the PD at every different speed, the results obtained using the iPD for which gains remained fixed are still better. Indeed, the iPD not only ensured the PD performance but also its augmented intelligent part adapted the local model resulting in cancelation of the perturbations and uncertainties, leading to better performances. In other words, once the gains K_p and K_d are fixed for the iPD to ensure stable closed-loop dynamics, the same gains are then used for the different ship speeds, providing satisfying results. The continuously updated term $(-\frac{F}{\alpha})$ captured all the structural information of the system dynamics to be canceled without the need of retuning the gains.

Table 4. MSI percentages at different speeds.

Speed(knots)	MSI PD%	MSI PD Scheduled gain%	MSI iPD%
20	6.57	4.72	3.56
30	8.12	6.80	3.82
40	8.31	8.31	4.2

5.3. Controller performances in different sea state numbers

The two controllers, classic and intelligent PD, were also tested for higher sea state numbers (SSN5 and SSN6). The resulting WVA signals are shown in Figures 14 and 15, and their corresponding MSI percentages are given in Table 5. It is clearly seen from the figures that at high sea state numbers the passengers experience an elevated WVA with mean values of 0.85 and 10.8 m/s^2 for SSN5 and SSN6, respectively, which are rough enough to induce seasickness in many passengers. Fortunately, at SSN5 the WVA is reduced by means of the controlled devices to reach 0.43 m/s^2 using the PD controller and 0.36 m/s^2 using the iPD controller. Once more, the iPD exhibited better performances than the PD controller. However, the results for SSN6 are quite similar for both controllers with 0.6 and 0.58 m/s^2 mean WVA using the PD and the iPD, respectively. This is due to the limitation in the actuators action where, for rough sea, they can only reduce a fraction of vertical motion. This tendency originates from the capacity of the actuator rather than from the tuning of the controller.

6. Conclusion

This study deals with the reduction in the vertical motions induced by random waves on a high-speed ferry and the amelioration of the comfort of its passengers using submerged T-foil and flaps. A new control law based on

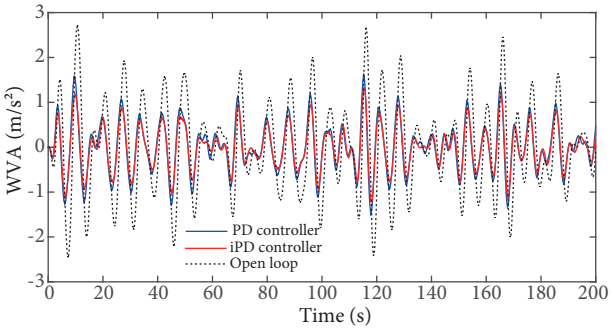

Figure 14. WVA response at 40 knots and SSN5.

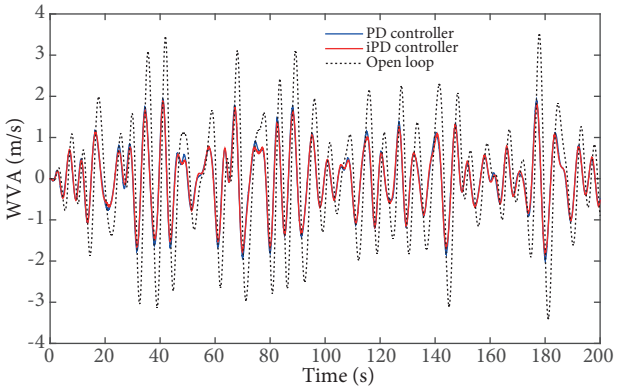

Figure 15. WVA response at 40 knots and SSN6.

Table 5. WVA and MSI percentages at different sea state numbers.

	WVA (m/s^2)			MSI (%)		
Sea state	Open loop	PD	iPD	Open loop	PD	iPD
4	0.74	0.41	0.30	22.50	8.31	4.20
5	0.85	0.43	0.36	26.74	9.13	6.40
6	10.8	0.60	0.58	36.23	16.01	15.53

a model-free strategy was designed to properly move the actuators where an intelligent PD controller has been utilized. A comparison between the classic PD and iPD was performed when encountering random sea waves. First, the tuning of the iPD gains showed a very direct way compared to the tuning of the classic PD, which is very dependent on the model. The results then showed that the iPD controller is very effective in eliminating the wave's disturbances better than the PD controller due to its ability to constantly reidentify the systems dynamics, leading to enhanced dynamic behavior and rejection of the perturbation. Indeed, the iPD exhibited a much better ability to handle the changing system parameters than the classic one when it demonstrates its model-free property. Furthermore, the two controllers were tested at different operating speeds and again the iPD showed its superiority over the classic PD. This serves as a good contribution for passengers' comfort and provides a baseline for further research with increased operational capabilities of the ship. This research study can be extended for testing different heading angles and introducing some adaptations to the controller in order to reach a global controller with better performances.

References

[1] Xi H, Sun J. Nonlinear feedback stabilization of high-speed planing vessels by a controllable transom flap. In: IEEE 2005 American Control Conference; 8–10 June 2005; Portland, OR, USA. New York, NY, USA: IEEE. pp. 4327-4332.

[2] Xi H, Sun J. Feedback stabilization of high-speed planing vessels by a controllable transom flap. IEEE J Oceanic Eng 2006; 31: 421-431.

[3] Esteban S, De la Cruz JM, Giron-Sierra JM, De Andres B, Diaz JM, Aranda J. Fast ferry vertical acceleration reduction with active flaps and T-foil. In: IFAC 5th Conference on Maneuvering and Control of Marine Crafts; 2000; Aalborg, Denmark. pp. 233-238.

[4] Giron-Sierra J, Esteban S, De Andres B, Diaz J, Riola J. Experimental study of controlled flaps and T-foil for comfort improvement of a fast ferry. In IFAC 2001 Proceedings of the International Conference on Control Applications in Marine Systems; July 2001; Glasgow, UK. pp. 261-266.

[5] Díaz J, Dormido S, Aranda J. Interactive computer-aided control design using quantitative feedback theory: the problem of vertical movement stabilization on a high-speed ferry. Int J Control 2005; 78: 813-825.

[6] Esteban S, Recas J, Giron-Sierra JM, De la Cruz J, Riola J. A fast autonomous scaled ship for experimental seakeeping control studies. In: IEEE Oceans 2005-Europe; 20–23 June 2005. New York, NY, USA: IEEE. pp. 1232-1237.

[7] Velasco F, López E, Rueda T, Moyano E. Classical controllers to reduce the vertical acceleration of a high-speed craft. In: IEEE 2003 European Control Conference; 1–4 September 2003; Cambridge, UK. New York, NY, USA: IEEE. pp. 1923–1927.

[8] De la Cruz JM, Aranda J, Giron-Sierra JM, Velasco F, Esteban S, Diaz JM. Improving the comfort of a fast ferry. IEEE Contr Syst Mag 2004; 24: 47-60.

[9] Aranda J, De la Cruz JM, Díaz J. Design of a multivariable robust controller to decrease the motion sickness incidence in fast ferries. Control Eng Pract 2005; 13: 985-999.

[10] Fliess M, Join C. Intelligent PID controllers. In: IEEE 2008 16th Mediterranean Conference on Control and Automation; 25–27 June 2008; Ajaccio-Corsica, France. New York, NY, USA: IEEE. pp. 326-331.

[11] Fliess M, Join C. Model-free control and intelligent PID controllers: towards a possible trivialization of nonlinear control? In: IFAC 15th Symposium on System Identification; 6–8 July 2009; Saint-Malo, France. pp. 1531-1550.

[12] D'Andréa-Novel B, Fliess M, Join C, Mounier H, Steux B. A mathematical explanation via "intelligent" PID controllers of the strange ubiquity of PIDs. In: IEEE 18th Mediterranean Conference on Control & Automation; 23–25 June 2010; Marrakech, Morocco. New York, NY, USA: IEEE. pp. 395-400.

[13] Åström KJ, Hang CC, Persson P, Ho WK. Towards intelligent PID control. Automatica 1992; 28: 1-9.

[14] Nagaraj B, Subha S, Rampriya B. Tuning algorithms for PID controller using soft computing techniques. International Journal of Computer Science and Network Security 2008; 8: 278-281.

[15] De Andres Toro B, Esteban S, Giron-Sierra J, De la Cruz JM. Modelling the motions of a fast ferry with the help of genetic algorithms. In: IMACS Symposium on Mathematical Modelling; 2–4 February 2000; Vienna, Austria. pp. 783-786.

[16] De la Cruz JM, Aranda J, Díaz J, Marrón A. Identification of the vertical plane motion model of a high speed craft by model testing in irregular waves. In: IFAC 1998 Conference of Control Applications in Marine Systems; 27–30 October 1998; Fukuoka, Japan. pp. 277-282.

[17] Esteban S, Giron-Sierra JM, De Andres-Toro B, De la Cruz JM, Riola J. Fast ships models for seakeeping improvement studies using flaps and T-foil. Math Comput Model 2005; 41: 1-24.

[18] Fossen TI. Guidance and Control of Ocean Vehicles. New York, NY, USA: John Wiley & Sons, 1994.

[19] O'Hanlon JF, MacCawley ME. Motion sickness incidence as a function of frequency and acceleration of vertical sinusoidal motion. J Sound Vib 1975; 41: 521.

[20] Fliess M, Join C. Model-free control. Int J Control 2013; 86: 2228-2252.

[21] Aranda J, Díaz J, Ruipérez P, Rueda T, López E. Decreasing of the motion sickness incidence by a multivariable classic control for a high speed ferry. In: IFAC 2001 International Conference of Control Applications in Marine Systems CAMS; 2001; Glasgow, UK.